New Phytologist

Research

Xylem formation can be modeled statistically as a function of primary growth and cambium activity

Jian-Guo Huang[1,2], Annie Deslauriers[2] and Sergio Rossi[2]

[1]Key Laboratory of Vegetation Restoration and Management of Degraded Ecosystems, South China Botanical Garden, Chinese Academy of Sciences, Guangzhou 510650, China; [2]Département de Sciences Fondamentales, Université du Québec à Chicoutimi, 555 Boulevard de l'Université, Chicoutimi, G7H 2B1, QC, Canada

Author for correspondence:
Jian-Guo Huang
Tel: +86 20 37081975
Email: huangjg@scbg.ac.cn

Received: *26 January 2014*
Accepted: *17 April 2014*

New Phytologist (2014) **203:** 831–841
doi: 10.1111/nph.12859

Key words: boreal forest, ecosystem, mixed-effects model, phenology, primary growth, secondary growth, tree growth, xylem formation.

Summary

- Primary (budburst, foliage and shoot) growth and secondary (cambium and xylem) growth of plants play a vital role in sequestering atmospheric carbon. However, their potential relationships have never been mathematically quantified and the underlying physiological mechanisms are unclear. We monitored primary and secondary growth in *Picea mariana* and *Abies balsamea* on a weekly basis from 2010 to 2013 at four sites over an altitudinal gradient (25–900 m) in the eastern Canadian boreal forest.
- We determined the timings of onset and termination through the fitted functions and their first derivative. We quantified the potential relationships between primary growth and secondary growth using the mixed-effects model.
- We found that xylem formation of boreal conifers can be modeled as a function of cambium activity, bud phenology, and shoot and needle growth, as well as species- and site-specific factors.
- Our model reveals that there may be an optimal mechanism to simultaneously allocate the photosynthetic products and stored nonstructural carbon to growth of different organs at different times in the growing season. This mathematical link can bridge phenological modeling, forest ecosystem productivity and carbon cycle modeling, which will certainly contribute to an improved prediction of ecosystem productivity and carbon equilibrium.

Introduction

Primary (e.g. budburst, foliage and shoot) growth and secondary growth (e.g. cambium differentiation and xylem formation) of plants play a vital role in sequestering atmospheric carbon. This role is particularly highlighted in an era of increasing atmospheric CO_2. Empirical phenological observations have recorded early budburst, shooting, leafing and flowering as a result of the recent early spring warming and extended growing season length (Chuine & Beaubien, 2001; Menzel *et al.*, 2006). Studies on cambium phenology have correspondingly revealed an early onset of cambium activity and xylem cell production as well as a longer duration of xylem formation (Huang *et al.*, 2011; Boulouf-Lugo *et al.*, 2012). Together these results suggest a potentially increasing role for primary and secondary growth in fixing carbon with climate warming.

Phenological models usually use phenological stages (timing of leafing, flowering, fruiting, and senescence) as model input parameters to fit and then predict tree species distribution under future climate change scenarios at a continental scale (Chuine & Beaubien, 2001; Morin *et al.*, 2007). Forest ecosystem productivity modeling and carbon cycle modeling often use primary growth (branch, foliage and root biomass) and secondary growth (ring width or diameter, growth or yield curve, or aboveground biomass) as inputs to assess and predict forest growth, ecosystem productivity and carbon equilibrium at regional to continental scales (Peng *et al.*, 2002; Pan *et al.*, 2011). However, it appears that these domains are relatively independent despite primary and secondary growth necessarily being connected. It is problematic to integrate phenological models into forest ecosystem productivity and carbon cycle modeling through parameterization given that there is no model to link phenological stages or timing with intra-annual cambium activity and xylem growth in the stem as a consequence of technical difficulties in collecting these data. Recent advances in wood anatomy made it possible to bridge this data gap (Deslauriers *et al.*, 2003) and to mathematically quantify the potential relationships between primary growth and intra-annual secondary growth. This quantification can link phenological modeling and ecosystem productivity modeling, which will certainly contribute to a more accurate assessment of ecosystem carbon equilibrium over both long (decadal to centennial) and short (seasonal to annual) time-scales, given a potentially increasing role for primary and secondary growth in fixing atmospheric carbon with climate warming.

Molecular biology has contributed to an improved understanding of the role of hormones in regulating cell division and growth (Fukuda, 2004) and of the stored forms and role of nonstructural carbon in trees during both the growing and

nongrowing seasons (Druart *et al.*, 2007; Carbone *et al.*, 2013). For example, it is generally assumed that the polar transport of auxin (e.g. indole-3-acetic acid (IAA)), which is produced from new buds, shoots and foliage in the canopy and translocated down the stem, triggers cambium cell differentiation that signals the onset of xylem formation and subsequently produces xylem wood (Savidge, 1988; Aloni, 2013). Nonstructural carbon such as stored starch, lipid or fat is considered to be the main source of energy for the onset of wood formation in early spring (Druart *et al.*, 2007). Evidence from molecular biology may therefore allow a better understanding and interpretation of the physiological mechanism linking primary to secondary growth.

In this study, we monitored primary and secondary growth in two dominant species, balsam fir (*Abies balsamea*) and black spruce (*Picea mariana*), at four sites along an altitudinal gradient in the boreal forest of Quebec, Canada from 2010 to 2013. We aimed to determine the timing of the onset and termination of growth in different organs using a novel approach; to mathematically quantify the potential relationships between cambium activity, xylem formation and primary growth over the altitudinal gradient; and to further elucidate the possible underlying mechanisms. We hypothesize that xylem formation can be modeled as a function of cambium activity and primary growth.

Materials and Methods

Field experiments and data collection

An uneven-aged natural boreal forest in the Parc National des Monts-Valins, Quebec, Canada was selected for the study, in which balsam fir (*Abies balsamea* (L.) Miller) and black spruce (*Picea mariana* (Mill.) B.S.P.) are the dominant species. Other species, such as white spruce (*Picea glauca* (Moench.)), birch (*Betula papyrifera* Marshall.) and aspen (*Populus tremuloides* Michx.), also occur, but with a reduced abundance toward high elevations. The regional climate is dominated by dry polar and moderate polar air masses in winter and by moist maritime and moist tropical air masses in summer (Sheridan, 2002). The 1961–1990 climate data from Bagotville meteorological station (159 m above sea level (a.s.l.); 10 km from the site) showed that the mean annual temperature was 2.2°C, with a maximum of 18°C in July and a minimum of −15.8°C in January. The mean annual temperature drops 0.6°C per 100 m elevation.

Spruce and fir trees were monitored during the 2010–2013 growing seasons at four sites: Saguenay (SA), Cibro (CI), Lagacé (LA) and Gaspard (GP), located from 25 to 900 m a.s.l. (Table 1). Primary growth measurements included bud phenology and needle and lateral shoot growth, while secondary growth measurements included cambium activity and xylem formation in the stem (Fig. 1). Three specimens per species/site were randomly selected from healthy, dominant or co-dominant trees. We excluded strongly suppressed trees and those with any signs of disease. Data were collected weekly from the beginning of May to the end of September during each of the four growing seasons. On each tree, four branches (two south-facing and two north-facing) were randomly selected from the canopy bottom and labeled as the monitored branches. Bud phenology stages were recorded weekly on each branch according to the seven-stage definition (Dhont *et al.*, 2010) but using a different numeration (closed bud (0), open bud (1), elongated bud (2), swollen bud (3), translucent bud (7), split bud (9) and exposed bud (10)) and a growing stage (11) (Fig. 1). Five needles and a lateral shoot per branch were randomly selected to measure weekly needle growth and shoot extension, respectively (Rossi *et al.*, 2009). A micro-core was extracted weekly from the stem at 1–1.3 m aboveground using Trephor (University of Padova, Padova, Italy) (Rossi *et al.*, 2006a).

The micro-core was then prepared in the laboratory and cut using a microtome to obtain a thin slice (7 μm thickness). Each slice was stained with cresyl violet acetate to identify different development phases of cambium cells and xylem cells (Fig. 1) (Deslauriers *et al.*, 2003). Three rows of cambium and xylem cells in each slice were selected to count the total number of cambium cells and xylem cells under the microscope.

Determination of onset and ending of primary and secondary growth

Given that xylem formation and shoot and needle growth over the growing season are characterized by an initial period of slow growth followed by an intermediate period of fast growth and then a final period of slow growth and can be well fitted by an S-shaped Gompertz function (Deslauriers *et al.*, 2003; Zhai

Table 1 Characteristics of the study sites (Lagacé (LA), Gaspard (GP), Saguenay (SA), and Cibro (CI)) and black spruce (*Picea mariana*) and balsam fir (*Abies balsamea*) stands

Species	Site	Latitude (°N)	Longitude (°W)	Elevation (m a.s.l.)	Stand age (yr) (mean, SD)	Height (m) (mean, SD)	Diameter at breast height (cm) (mean, SD)	Data collection
Spruce	LA	48.60	70.83	900	73 (20.3)	4.6 (1.04)	14 (0.03)	2010–13
	GP	48.58	70.88	227	40 (3.7)	14.2 (1.6)	24.7 (1.4)	2010–13
	SA	48.44	70.88	25	48 (6.2)	6.1 (2.1)	10.3 (3.5)	2011–13
	CI	48.44	70.90	72	25 (4.1)	5.1 (1.4)	6.6 (2.6)	2010
Fir	LA	48.60	70.83	900	25 (2.5)	7.6 (0.7)	16.8 (4.0)	2010–13
	GP	48.58	70.88	227	50 (3.7)	17.6 (2.6)	32.2 (9.1)	2010–13
	SA	48.44	70.88	25	49 (2.9)	10.7 (1.6)	14.7 (4.2)	2011–13
	CI	48.44	70.90	72	28 (2.5)	6.8 (2.3)	8.0 (1.5)	2010

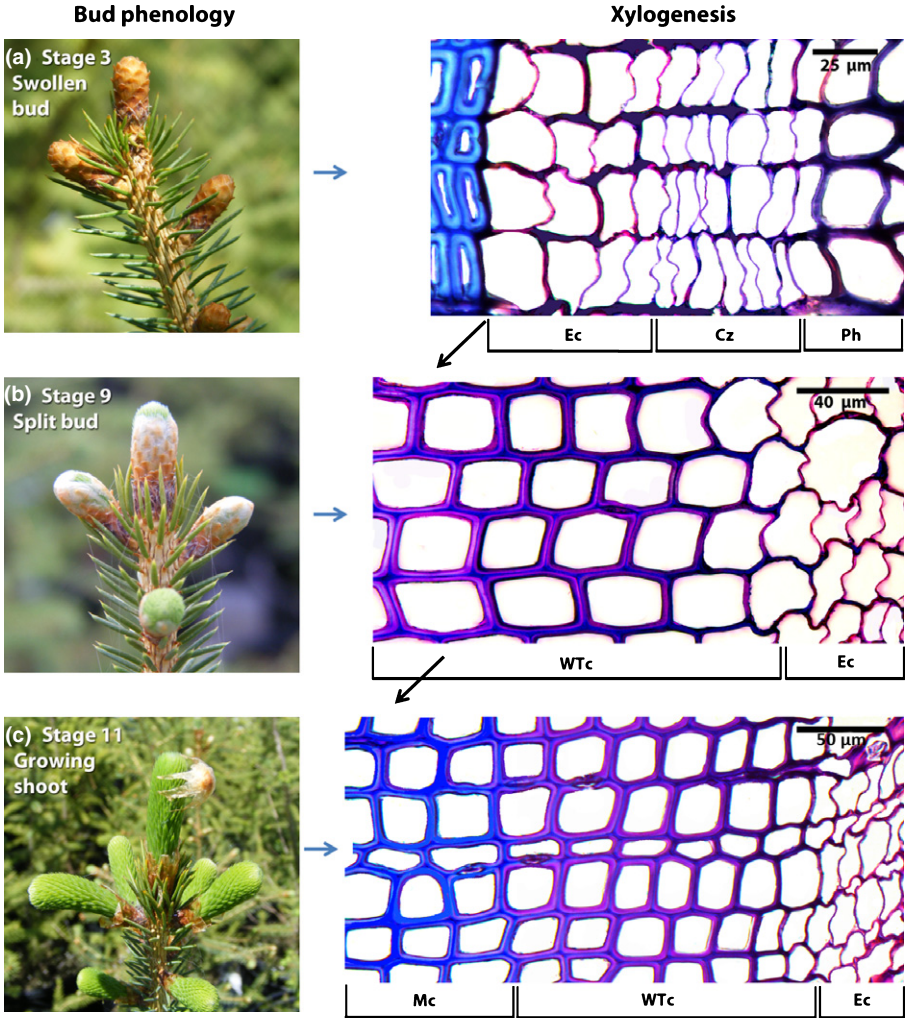

Fig. 1 Illustration of some stages of bud break with the corresponding status of xylem development in black spruce (*Picea mariana*) located at Gaspard (GP). (a) At the end of May, a swelling bud is evident. The scales of the upper part of the bud are smooth and pale colored but no needles are visible. At this time, cambium activity has already begun (indicated by an increase in the number of cells that compose the cambial zone) with no or very few xylem cells in the enlargement phase. (b) At the beginning of June, the new shoot has undergone elongation but the needles are still tightly clustered in the buds. The tops of the needles are apparent. In the meantime, some enlarging cells have undergone the cell wall thickening phase while new enlarging cells are still produced by the cambium. (c) When the shoot is actively growing at the end of June, several cells have reached maturity (Mc) and the rate of wood formation starts to decline. Ph, phloem; Cz, cambial zone; Ec, enlarging cells; WTc, wall thickening cells; Mc, mature cells. (Photos of budburst from Ms Lorena Balducci).

et al., 2012), we first fitted xylem cell number, needle length, shoot length, and bud phenology stages using the Gompertz function to estimate the parameters (Supporting Information Fig. S1 and Table S1). The 95% Wald confidence interval was also calculated. The timing of the onset of growth of these organs was then directly calculated from the Gompertz function, setting xylem cell number at 1, needle length at 0.1 mm, shoot length at 0.1 mm, and bud phenology stage at 1. Given their S-shaped behavior, the instantaneous growth rate on day t of the year, that is, the first derivative of the Gompertz function, should be a normal curve. The instantaneous rate of growth for xylem, shoot and needle at the timing of termination should be equal to that at the timing of onset. The time of termination can therefore be determined as the day on which the growth rate in the final growth period is approximately equal to that on the day of growth onset (Methods S1).

For the cambium, the active period was determined from the first derivative of the Hugershoff function, which is a generalized exponential function (Warren, 1980; Methods S1, Fig. S2, Table S2). Theoretically, the activity of cambium cells (four cells on average) remains constant in the dormant period during winter, then increases in early spring and decreases in summer and autumn, and the cells once again enter the dormant state in winter (Rossi *et al.*, 2006b). We therefore expected to determine the timing and duration of increased cambium activity in early spring, which is potentially related to its capacity to gather auxin and divide cells.

Mixed-effects model

We used a mixed-effects model to fit our hierarchical data, in which an autocorrelation error structure in the repeated

measurements over time was extended to level 1 (AR(1), first order autoregressive errors) which was nested within the observations of the organs (level 2) and within trees (level 3), across species (level 4) and sites or elevations (level 5) (Fig. S3). In addition, there was a nested error structure, that is, correlation among trees within species\sites. The mixed-effects model can effectively deal with this nested error structure to account for correlation associated with clustered data. Mixed-effects model techniques estimate fixed and random parameters simultaneously and give unbiased and efficient estimates of fixed parameters (Pinheiro & Bates, 2000). In our mixed-effects model, fixed effects included weekly cambium cell number, bud phenology stages, needle growth and shoot growth, species, site or elevation, and species × site interactive effects. Random effects included trees and repeated observations over time. A conventional mixed-effects model-building process (Singer, 1998) was used starting from a null model and then gradually extending to the higher levels (Fig. S4). We assumed that xylem formation in a tree during a growing season may be modeled as a function of cambium activity, bud phenology stages, needle and shoot growth, species effects, site effects, and site × species interactive effects, as well as random effects. It can theoretically be expressed as

$$\begin{aligned} Y_{i(jklt)} = {} & \beta_0 + \left(\beta_1 + \mu_{1j}\right) C_{i(jklt)} + \left(\beta_2 + \mu_{2j}\right) P_{i(jklt)} \\ & + \left(\beta_3 + \mu_{3j}\right) N_{i(jklt)} + \left(\beta_4 + \mu_{4j}\right) S_{i(jklt)} + \beta_5 \mathrm{Sp}_{k(l)} \\ & + \beta_6 E_l + \beta_7 \mathrm{Sp}_{k(l)} E_l + \mu_{0j} + \varepsilon_{i(jklt)} \end{aligned} \qquad \text{Eqn 1}$$

($Y_{i(jklt)}$, the ith (i = 1–3) observed xylem cell number in the jth tree (j = 1–3) of the kth species in the lth site on day t; β_0, the overall mean; β_1, β_2,... and β_7, the corresponding fitted parameters; $C_{i(jklt)}$, the ith (i = 1–3) observed cambium cell number in the jth tree of the kth species in the lth site on day t; $P_{i(jklt)}$, the observed bud phenological stage in the ith (i = 1–4) branch on the jth tree of the kth species in the lth site on day t; $N_{i(jklt)}$, the ith (i = 1–20) measured needle length (mm) on the jth tree of the kth species in the lth site on day t; $S_{i(jklt)}$, the measured length (mm) of the ith (i = 1–4) shoot on the jth tree of the kth species in the lth site on day t; $\mathrm{Sp}_{k(l)}$, the kth (k = 1 for spruce or 0 for fir) species in the lth site; E_l, the elevation of the lth site (l = 1 for CI, 2 for SA, 3 for GP and 4 for LA); $\mathrm{Sp}_{k(l)} \times E_l$, the interactive effects of the kth species in the lth site; μ_0, random intercept; μ_1, μ_2, μ_3, and μ_4, random slopes,

$$\text{where} \begin{pmatrix} \mu_0 \\ \mu_1 \\ \mu_2 \\ \mu_3 \\ \mu_4 \end{pmatrix} \sim N\left[\begin{pmatrix} 0 \\ 0 \end{pmatrix}, \begin{pmatrix} \tau_{00} & \tau_{01} \\ \tau_{10} & \tau_{11} \end{pmatrix}\right], \qquad \text{Eqn 2}$$

τ_{00} and τ_{11}, the elements representing the variance components for the intercept and slope, respectively; τ_{10}, the covariance component representing correlation between the intercept and slope.)

$\varepsilon_{i(jklt)}$ is the random error associated with the ith observation on the jth tree of the kth species in the lth site on day t; $\varepsilon_{i(jklt)} \sim N(0, \sigma_\varepsilon^2 \Omega)$, where

$$\sigma_\varepsilon^2 \Omega = \frac{\sigma_\varepsilon^2}{(1-\rho^2)} \begin{bmatrix} 1 & \rho & \rho^2 & \dots & \rho^{n-1} \\ \rho & 1 & \rho & \dots & \rho^{n-2} \\ \rho^2 & \rho & 1 & \dots & \rho^{n-3} \\ . & . & . & \dots & . \\ \rho^{n-1} & \rho^{n-2} & \rho^{n-3} & \dots & 1 \end{bmatrix}, \qquad \text{Eqn 3}$$

and ρ is the autocorrelation coefficient, $|\rho| < 1$.

Statistical analysis

Square root transformation of the number of xylem and cambium cells was conducted to meet the assumption of normality. Bud phenology stages also underwent square root transformation for further modeling analysis. Note that hereinafter the transformed data were used in the mixed-effects model analysis. Before the modeling analysis, variance inflation factors (VIFs) (Belsley *et al.*, 1980) were also calculated to detect multicollinearity among the predictors. The predictors included the square root of cambium cell number, needle growth, shoot growth, the square root of bud phenology stages, and elevation. VIFs were generally lower (< 3) than the accepted value of 4 (O'Brien, 2007).

The mixed-effects model was built according to the conventional building process (Singer, 1998); the detailed mathematical or statistical approaches used can be found in Methods S2.

To provide an absolute value for the goodness of fit of a mixed-effects model as routinely reported in a generalized linear model, Nakagawa & Schielzeth (2013) recently reported a marginal R^2, calculated on the fixed effects only, and a conditional R^2, calculated on both fixed and random effects. We therefore calculated them to assess the overall performance of a mixed-effects model (Methods S3). To provide information regarding the variance explained at each level, the proportion change in variance (PCV; Merlo *et al.*, 2005) was calculated (Methods S3). The assumption of normality of the residuals was also verified. Sensitivity analysis (SA), which attempts to provide a ranking of the model inputs based on their relative contributions to the model output variability and uncertainty (Cariboni *et al.*, 2007), was conducted to determine which parameters have the greatest effect on the model output. The SA approach, in which the model parameters are varied one at a time, was used and the model parameters were perturbed with two standard deviations. In addition, decomposition of variance (DOV) (Huang *et al.*, 2013) was performed to further quantify how much variance in the predicted square root of xylem cell number can be attributed to different fixed-effects predictors using SAS Proc GLM (type III). All analyses were conducted using SAS (version 9.2; SAS Institute Inc., Cary, NC, USA).

Results

Onset and termination of growth of different organs

Primary growth and xylem formation (except for some organs in CI) were well fitted by the Gompertz function, as indicated by high adjusted R^2 (Fig. S1, Table S1). Cambium activity (except in SA and CI) was also fitted by the Hugershoff function (Fig. S2, Table S2). The failure of the model fit for the sites mentioned above was a consequence of a lack of sufficient data. The onset and termination of growth of different organs were determined (Table S1). As expected, growth rates of all organs, except for the cambium, showed a normal curve during the growing season and peaked around mid-June to the end of June (Fig. 2). The cambium showed a decreasing growth rate over the growing season. Overall, the general trend was that trees at lower sites started growth earlier than those at higher sites. Correspondingly, the growth rate peaked 2–3 wk earlier at lower sites than at higher

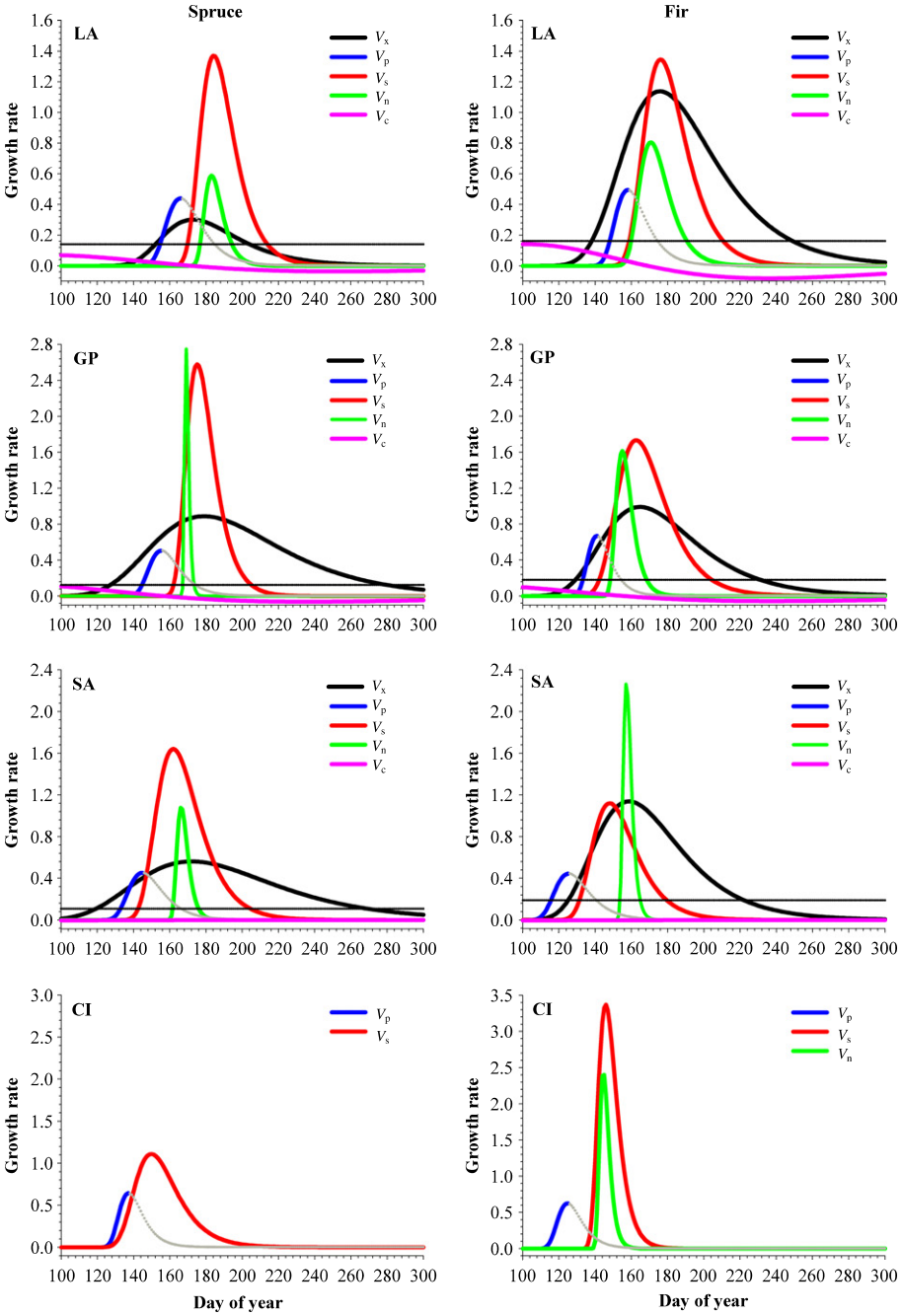

Fig. 2 Growth rate over time for different organs (xylem (V_x, number of cells), bud phenology (V_p, stage), shoot (V_s, cm), needle (V_n, cm), and cambium (V_c, cell number)) for spruce (left column) and fir (right column) over the altitudinal gradient or sites (Lagacé (LA), Gaspard (GP), Saguenay (SA), and Cibro (CI)). The solid line indicates the growth rate (V_x) when the xylem cell number equals 1. Growth rate data were not available for some organs in CI. The gray line indicates the right half of the normal curve for bud phenology stages, which is meaningless (*n* equals df in Supporting Information Tables S1 and S2).

sites. In terms of the growth order of different organs, the cambium became intensively active in early spring, which triggered the subsequent onset of xylem formation. Xylem formation generally preceded bud phenology, followed by shoot growth and then needle growth (except in SA). Depending on the site, xylem formation ended in mid-August to mid-September, after the termination of shoot growth, which occurred around the end of July to mid-August. In addition, the maximum xylem growth rate for both species occurred roughly a few days before or after the summer solstice. Fir generally started growth 1–3 wk earlier than spruce at the same site, varying by organs. The maximum xylem growth rate was generally higher for fir than for spruce. For the duration of growth, bud phenology was shortest, followed by needle, shoot and xylem.

Full model

As indicated by the intra-class correlation coefficient (ICC) in Table 2, 15.26% of the variability in xylem formation was explained by the two-level random effects, emphasizing the importance of accounting for the hierarchical structure of the data. The full model was considered the best model in terms of minimum Akaike Information Criterion (AIC) and Bayesian Information Criterion (BIC). It included both fixed effects and random intercept effects. Random slopes (μ_1 to μ_4 in Eqn 1) were excluded because they were statistically insignificant. The full model demonstrated that xylem formation is a function of cambium activity, bud phenology stages, needle and shoot growth, species, elevation, and species × elevation interactive effects, as well as random intercept effects and an autocorrelation error term. It was given by

$$\sqrt{Y_{i(jklt)}} = \beta_0 + \beta_1\sqrt{C_{i(jklt)}} + \beta_2\sqrt{P_{i(jklt)}} + \beta_3 N_{i(jklt)} + \beta_4 S_{i(jklt)} + \beta_5 \mathrm{Sp}_{k(l)} + \beta_6 E_l + \beta_7 \mathrm{Sp}_{k(l)} E_l + \mu_{0j} + \varepsilon_{i(jklt)} \quad \text{Eqn 4}$$

where the variables and parameters are described in Eqn 1, μ_{0j} is assumed to be normally distributed with mean of zero and variance of δ^2_{tree}.

Given that the onset of xylem formation preceded bud phenology followed by shoot and needle growth, the full model was conditional upon the square root of xylem cell number being greater than zero. It performed well in explaining the total variance in the square root of xylem cell number using both fixed

Table 2 Statistics for the null model and full model as well as the decomposition of variance (DOV) in the predicted xylem cell number using fixed effects only

Model	Null model (×10^{-2})	Full model (×10^{-2})	DOV (%)
Fixed effects			
Intercept (β_0)	555.70 (34.16)***	−176.26 (36.82)***	
Cambium cell number (β_1)		65.18 (10.18)***	7.06
Bud phenology, stage (β_2)		83.54 (5.25)***	43.07
Needle length (β_3)		9.90 (1.09)***	13.89
Shoot length (β_4)		3.13 (0.31)***	16.99
Species (spruce) (β_5)		104.37 (14.85)***	8.74
Species (fir)		0	
Elevation (β_6)		0.11 (0.02)***	0.08
Species × elevation (spruce) (β_7)		−0.20 (0.03)***	10.17
Species × elevation (fir)		0	
Random effects			
Residuals	691.66 (28.28)***	140.99 (7.29)***	
Tree (species × site)	64.05 (37.39)*	0.25 (0.82)	
Observation (tree) (AR(1))	60.48 (1.64)***	3.93 (4.04)	
ICC (observation)	7.41%		
ICC (tree)	7.85%		
PCV (observation)		93.50%	
PCV (tree)		99.61%	
PCV (residuals)		79.62%	
R^2_marginal (spruce)		0.71	
R^2_conditional (spruce)		0.72	
R^2_marginal (fir)		0.74	
R^2_conditional (fir)		0.75	
Model fit			
−2 log likelihood	10294.3	2414.8	
AIC	10302.3	2436.8	
AICC	10302.4	2437.1	
BIC	10294.3	2414.8	

AIC, Akaike Information Criterion; AICC, The corrected Akaike Information Criterion; AR(1), first order autoregressive errors; BIC, Bayesian Information Criterion; ICC, intra-class correlation; PCV, proportion change in variance.
Standard error (SE) is given in brackets.
***, $P < 0.0001$; *, $P < 0.05$.

and random effects as suggested by the evenly distributed residuals over zero (Fig. S5) and the high marginal and conditional R^2 (Table 2). Fixed effects alone explained the majority of the total variability in the square root of xylem cell number (marginal $R^2 = 0.71$ for spruce and 0.74 for fir), while the random effects accounted for only minor variance (< 1%). The full model also performed well in explaining the total variance at each level, as indicated by high PCV (Table 2). Only 25% for spruce and 28% for fir of the total variability in the square root of xylem cell number could not be explained. As shown in Fig. 3, xylem cell

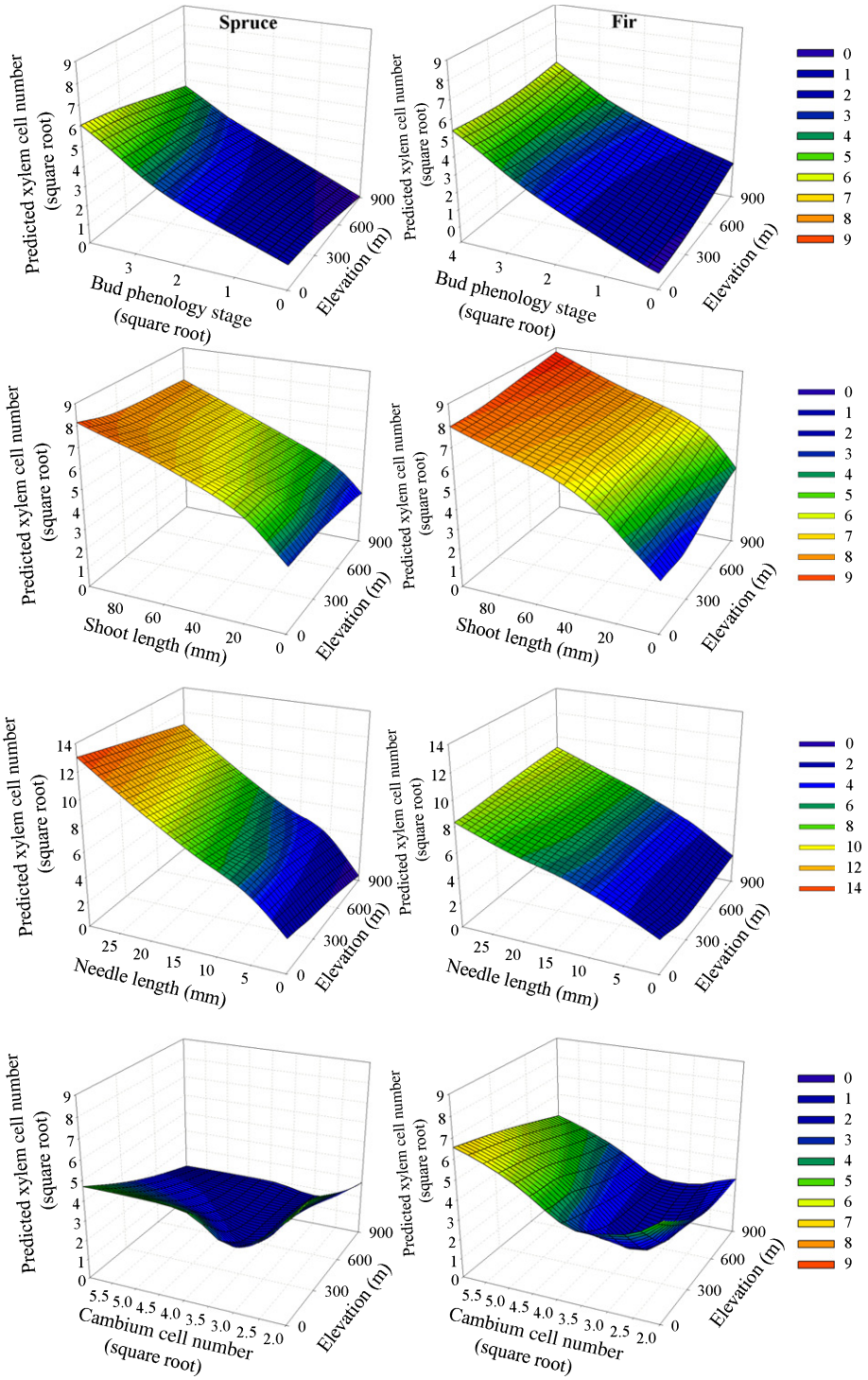

Fig. 3 Surface plot (after smoothed spline interpolation based on $n = 348$ for spruce and $n = 406$ for fir) showing the relationships between the predicted xylem cell number (square root) and bud phenology stage (square root), shoot growth, needle growth, and cambium cell number (square root) for spruce (left column) and fir (right column) during the growing seasons over the altitudinal gradient.

number increased when the cambium became active, following which bud phenology proceeded, with subsequent growth extension of shoots and needles during the growing season.

SA showed that bud phenology (*c.* 29%) was ranked as the most important and sensitive variable; shoot growth and needle growth were in turn ranked as the second (*c.* 26%) and third (*c.* 24%) most sensitive variables, respectively, while elevation (10–12%) and cambium activity (10–11%) were the two least sensitive variables (Fig. 4). This ranking was further confirmed by the DOV results, in which 43% of the variability in the predicted square root of xylem cell number could be explained by the square root of bud phenology, followed by shoot (17%) and needle growth (14%), as well as elevation (*c.* 10%) and square root of cambium activity (7%) (Table 2).

Discussion

It has long been assumed that primary growth and secondary growth are synchronized over the growing season (Larson, 1964). In this study, we first mathematically quantified the potential relationships between primary growth and secondary growth for spruce and fir over the growing seasons in the Canadian boreal forest. We found, however, that primary growth and secondary growth are not synchronized at the beginning of wood formation, whereas they become synchronized after budburst, as demonstrated by the model. This implies that primary growth does not regulate the onset of wood formation in boreal conifers. Budburst appears to be a critical point separating the total period of wood formation into two different phases, that is, before and after budburst, during which the source of energy for wood formation switches from carbon stored previously and produced by older needles to carbon generated by the newly formed structures (see later discussion).

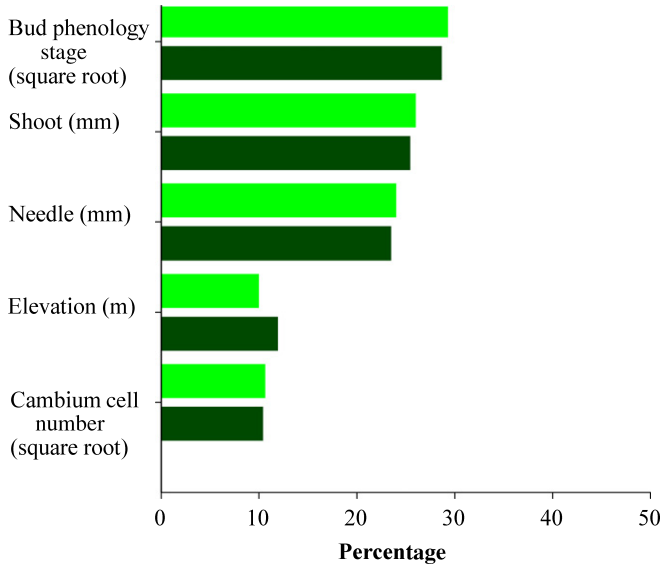

Fig. 4 Ranking of the model input parameters (bud phenology stage, shoot growth, needle length growth, elevation and cambium cell number) based on the percentage contribution of each parameter to the total variability in the square root of xylem cell number for spruce (light green) and fir (dark green) when each parameter (base case) was disturbed by 2 standard deviations individually using sensitivity analysis.

Xylem formation is a complex process that is regulated by both endogenous (i.e. hormones and sugars) and exogenous (i.e. photoperiod, temperature, water availability and nutrients) factors. Xylem cell formation results from cell proliferation within stem cells, such as the procambium and cambium, contained in the vascular meristem (Fukuda, 2004). This process is mediated by phytohormones that are produced by developing buds, shoots, foliage and roots. These compounds play a role in integrating environmental signals and regulating cell development when exogenous factors are not limited in spring (Matsumoto-Kitano *et al.*, 2008). We quantified this complex relationship through modeling xylem formation as a function of cambium activity, bud phenology, and shoot and needle growth, as well as species and site-specific factors. That said, a direct mathematical link between wood formation and primary growth was established first, given that the majority of variance (74%) in the predicted xylem cell production (conditional $R^2 \geq 0.72$) was explained by primary growth. This link can allow better integration of phenological modeling into forest growth, ecosystem productivity and carbon cycle modeling through parameterization because primary growth is the basic input variable for the former, whereas ring growth is one of the basic input variables for the latter. It can also provide more parameters describing the mathematical relationships between wood formation and other tree organs for a better understanding of tree growth processes to improve the definition of process-based models such as the process-based standardization (PBS) model (Melvin, 2004).

Physiological mechanisms

Given that the total period of wood formation was divided into two phases, that is, before and after budburst, we further elucidated the physiological mechanisms underlying these two phases. In terms of spring temperature, our results indicate different temperature thresholds triggering the onset of primary and secondary growth. This finding is in contrast to that of Aloni (2001), who reported that budburst and foliage development are related to cambial reactivation and xylem differentiation, but is consistent with that of Begum *et al.* (2013), who found that a close relationship does not always exist between the timing of budburst and cambial reactivation. The discrepancy may be attributable to species and site differences.

Both cambium activity and the onset of xylem formation occurred before budburst in the two species, which is consistent with other boreal (Zhai *et al.*, 2012) and European (Rossi *et al.*, 2009) conifers. The start of wood formation before budburst thus indicates an alternative source of energy and carbon skeletons during this period (Begum *et al.*, 2013). The enzyme-mediated conversion of the stored starch into sugars and the lipid droplets in the cambium might be used as energy sources for cambial activity and the initiation of wood formation (Begum *et al.*, 2013). Sucrose catabolism generates hexoses that can be metabolized via glycolysis, while fats are metabolized via beta-oxidation and the glyoxylate cycle during cambial reactivation in spring (Druart

et al., 2007). In early spring, in addition to the stored energy, the newly formed photosynthates in old needles also provide certain sources of energy before the current-year needles develop (Oleksyn *et al.*, 2000). During this phase, auxin, which originates from the dormant shoot tips or buds, is essential for cambium reactivation and may supply positional information to the cambium, because an extremely low auxin concentration can stimulate the reactivation of the cambium, as shown in ring-porous species (Aloni, 2001). Auxin is considered to be a spatial mediator for cambium activity but a temporal regulator for xylem formation (Matsumoto-Kitano *et al.*, 2008). Cytokinins, which are often produced in meristematic zones such as roots, are also believed to be the central regulators for cambial activity if the meristem is supplied with an optimal concentration of auxin: both hormones control the activity of cyclin-dependent protein kinases (CDKs) regulating the cell division cycle, especially progression through the G1–S and G2–M phases (den Boer & Murray, 2000).

The model demonstrated that xylem formation after budburst was positively associated with bud phenology, shoot growth, needle growth and cambium activity, suggesting that xylem formation was mainly determined by the development of primary growth and cambium activity over the growing season. The effect of primary growth was also seen in an approximate synchronization in maximum growth rate between primary growth and xylem formation (Fig. 2). Growth peaks observed before or shortly after the summer solstice, when day length was longest, agree with Rossi *et al.* (2006b). This consistency suggests that trees, regardless of site and species differences, must follow a biological clock to grow by perceiving the changes in day length during the growing season. This self-control mechanism may allow trees to complete growth within a limited growing season and to be well prepared for the coming winter. Photoperiod or day length is believed to be a key factor in regulating plant growth (Jackson, 2008). Starch reserves in leaves are greater during the longer days (Zeeman *et al.*, 2007) which also favor transitory starch degradation (i.e. starch stored during the day in chloroplasts and broken down at night for export; Lu *et al.*, 2005), thus providing a source of carbon to support sucrose synthesis, respiration and growth at night.

Among the measured organs, bud phenology was ranked as the most important variable, indicating that budburst may determine much of wood formation through a continuous supply of hormones when wood formation has already started. Although developing shoots and foliage are hidden in developing buds at this stage, these developing organs are the major source organs of auxin, which can be basipetally transported to the cambium and xylem to promote cambial cell division and xylogenesis (Aloni, 2001). Auxin is considered the primary hormonal signal among those involved in the regulation of cambium activity and cell differentiation. Given that the major path of auxin is located in the cambium, the continuous polar transport of this compound along the stem will induce vascular differentiation in coordination with other hormones and regulatory molecules (see review by Sorce *et al.*, 2013). Our results thus support the proposal that xylem development can be used as an anatomical expression of auxin transport and directly link to bud phenology.

Developing shoots and needles, as the second and third most important variables, respectively, might not only continuously supply auxin at high concentrations, but also export more sucrose for xylem growth during development. The mechanism of growth requires sucrose for many processes (Muller *et al.*, 2011): to supply energy for division, to generate water turgor pressure during cell expansion and to produce polysaccharides during cell-wall formation. The optimum allocation theory stipulates that trees modify their allocation pattern to capture the resource that most limits growth (Poorter & Navas, 2003). Shoot growth of shade-tolerant species is critical to accommodate new needles and maximize the photosynthetic apparatus and capacity to capture light for growth, as observed in shade-tolerant boreal conifers (Claveau *et al.*, 2005). Net photosynthetic rate in *Picea sitchensis* was reported to increase more rapidly during needle expansion than either chlorophyll concentration or the activity of ribulose-1,5-bisphosphate carboxylase (Chandler & Dale, 1993). In addition, carbon allocation studies found that there is a preferential use of newer nonstructural carbon (fast pool) for day-to-day metabolism and growth, whereas, given other physiological constraints, the older nonstructural carbon (slow pool) remains accessible to the tree (Carbone *et al.*, 2013). A tree-ring isotope ($\delta^{13}C$)-based study revealed that latewood was mainly composed of photoassimilates formed during the current summer and autumn (Kagawa *et al.*, 2006). These studies support our findings of positive relationships between needle growth and xylem formation reflected in the model.

The cambium is the meristem responsible for cell division and is a sink organ of carbon. It may play a role in regulating xylem formation, as indicated by its ranking. Cambium activity requires a continuous supply of energy to produce xylem cells, and the cambium can therefore be simply regarded as a 'factory'. A previous study reported that the cambium growth rate is associated with leaf biomass (Uggla *et al.*, 1998). However, we found that this was not the case in our study because the cambium growth rate peaked before the onset of xylem formation, whereas the maximum rate of growth in needle length occurred in June and therefore the needle biomass peak may lag behind as a result of continuous growth in needle width and weight.

Species differences over the altitudinal gradient

Overall, fir generally started growth earlier than spruce, which might be attributed to genetic differences because species' capacity to perceive exogenous signals such as spring temperature is mediated by hormones (Aloni, 2001). Earlier onset of growth observed for trees at lower elevations than at higher elevations was attributable to earlier spring warming at lower sites (Moser *et al.*, 2010). This trend is also consistent with that observed over the latitudinal gradient (Huang *et al.*, 2011). The slower xylem growth rate with an earlier peak, compared with needle and shoot growth rates, for spruce at the highest site may be attributable to both the harsher growing conditions and the presence of old stands. Spruces on the mountain top are dwarf but old, and foliage and branch losses were observed due to wind and snow abrasion.

In summary, based on a 4-yr experiment monitoring the primary and secondary growth of spruce and fir on a weekly basis over an altitudinal gradient in eastern Canada, we first mathematically quantified the potential relationships between primary growth and secondary growth. A striking finding was that xylem formation can be modeled as a function of cambium activity, bud phenology, shoot elongation, needle growth, and site- and species-specific factors. This finding also reveals that, after budburst, primary growth and secondary growth were synchronous over the growing season in boreal conifers, indicating that there may be an optimal mechanism to simultaneously allocate photosynthetic products and stored nonstructural carbon to the growth of different organs in trees. We foresee that this pioneer study will initiate an era of quantifying the relationships between primary growth and secondary growth, which will certainly contribute to an improved prediction of forest ecosystem productivity and carbon cycling when phenological models are incorporated through the parameterization between primary and secondary growth.

Acknowledgements

This project was funded by the Natural Sciences and Engineering Research Council of Canada (NSERC). J-G.H. received funding from Canada Mitacs-Accélération Québec-Programme de Stages de Recherche, Produits forestiers Résolu, and the 100 Talents Program of the Chinese Academy of Sciences (CAS) and South China Botanical Garden of the CAS (201401). We thank statistics expert Dr M. Mazerolle (UQAT) for discussion on the mixed-effects model. Special thanks are due to Claude Pelletier from the Parc national des Monts-Valin and Germain Savard for their help with data collection.

References

Aloni R. 2001. Foliar and axial aspects of vascular differentiation: hypotheses and evidence. *Journal of Plant Growth Regulation* **20**: 22–34.

Aloni R. 2013. Role of hormones in controlling vascular differentiation and the mechanism of lateral root initiation. *Planta* **238**: 819–830.

Begum S, Nakaba S, Yamagishi Y, Oribe Y, Funada R. 2013. Regulation of cambial activity in relation to environmental conditions: understanding the role of temperature in wood formation of trees. *Physiologia Plantarum* **147**: 46–54.

Belsley DA, Kuh E, Welsch RE. 1980. *Regression diagnostics: identifying influential data and sources of collinearity*. New York, NY, USA: John Wiley & Sons.

den Boer BGW, Murray JAH. 2000. Triggering the cell cycle in plants. *Trends in Cell Biology* **10**: 245–250.

Boulouf-Lugo J, Deslauriers A, Rossi S. 2012. Duration of xylogenesis in black spruce lengthened between 1950 and 2010. *Annals of Botany* **110**: 1099–1108.

Carbone MS, Czimczik CI, Keenan TF, Murakami PF, Pederson N, Schaberg PG, Xu X, Richardson AD. 2013. Age, allocation and availability of non-structural carbon in mature red maple trees. *New Phytologist* **200**: 1145–1155.

Cariboni J, Gatelli D, Liska R, Saltelli A. 2007. The role of sensitivity analysis in ecological modelling. *Ecological Modelling* **203**: 167–182.

Chandler JW, Dale JE. 1993. Photosynthesis and nutrient supply in needles of Sitka spruce [*Picea sitchensis* (Bong.) Carr.]. *New Phytologist* **125**: 101–111.

Chuine I, Beaubien E. 2001. Phenology is a major determinant of temperate tree range. *Ecology Letters* **4**: 500–510.

Claveau Y, Messier C, Comeau P. 2005. Interacting influence of light and size on aboveground biomass distribution in sub-boreal conifer saplings with contrasting shade tolerance. *Tree Physiology* **25**: 373–384.

Deslauriers A, Morin H, Begin Y. 2003. Cellular phenology of annual ring formation of *Abies balsamea* in the Quebec boreal forest (Canada). *Canadian Journal of Forest Research* **33**: 190–200.

Dhont C, Sylvestre P, Gros-Louis MC, Isabel N. 2010. *Field guide for identifying bud break and bud formation stage in white spruce*. Ottawa, ON, Canada: Natural Resources Canada.

Druart N, Johansson A, Baba K, Schrader J, Sjödin A, Bhalerao RR, Resman L, Trygg J, Moritz T, Bhalerao RP. 2007. Environmental and hormonal regulation of the activity-dormancy cycle in the cambial meristem involves stage-specific modulation of transcriptional and metabolic networks. *Plant Journal* **50**: 557–573.

Fukuda H. 2004. Signals that control plant vascular cell differentiation. *Nature Reviews Molecular Cell Biology* **5**: 379–391.

Huang JG, Bergeron Y, Berninger F, Zhai LH, Tardif J, Denneler B. 2013. Impact of future climate on radial growth of four major boreal tree species in the eastern Canadian boreal forest. *PLoS ONE* **8**: e56758.

Huang JG, Bergeron Y, Zhai LH, Denneler B. 2011. Variation in intra-annual radial growth (xylem formation) of *Picea mariana* (Pinaceae) along a latitudinal gradient in western Quebec, Canada. *American Journal of Botany* **98**: 792–800.

Jackson SD. 2008. Plant responses to photoperiod. *New Phytologist* **181**: 517–531.

Kagawa A, Sugimoto A, Maximov TC. 2006. $^{13}CO_2$ pulse-labelling of photoassimilates reveals carbon allocation within and between tree rings. *Plant, Cell & Environment* **29**: 1571–1584.

Larson PR. 1964. Contribution of different-aged needles to growth and wood formation of young red pines. *Forest Science* **10**: 224–238.

Lu Y, Gehan JP, Sharkey TD. 2005. Daylength and circadian effects on starch degradation and maltose metabolism. *Plant Physiology* **138**: 2280–2291.

Matsumoto-Kitano M, Kusumoto T, Tarkowski P, Kinoshita-Tsujimura K, Václaviková K, Miyawaki K, Kakimoto T. 2008. Cytokinins are central regulators of cambial activity. *Proceedings of the National Academy of Sciences, USA* **105**: 20027–20031.

Melvin TM. 2004. *Historical growth rates and changing climatic sensitivity of boreal conifers*. PhD thesis, Climate Research Unit, School of Environmental Sciences, University of East Anglia, Norwich, UK.

Menzel A, Sparks TH, Estrella N, Koch E, Aasa A, Ahas R, Alm-Kübler K, Bissolli P, Braslavska O, Briede A *et al.* 2006. European phonological response to climate change matches the warming pattern. *Global Change Biology* **12**: 1969–1976.

Merlo J, Chaix B, Yang M, Lynch J, Rastam L. 2005. A brief conceptual tutorial on multilevel analysis in social epidemiology: interpreting neighbourhood differences and the effect of neighbourhood characteristics on individual health. *Journal of Epidemiology & Community Health* **59**: 1022–1028.

Morin X, Augspurger C, Chuine I. 2007. Process-based modeling of species' distributions: what limits temperate tree species' range boundaries? *Ecology* **88**: 2280–2291.

Moser L, Fonti P, Büntgen U, Esper J, Luterbacher J, Franzen J, Frank D. 2010. Timing and duration of European larch growing season along altitudinal gradients in the Swiss Alps. *Tree Physiology* **30**: 225–233.

Muller B, Pantin F, Genard M, Turc O, Freixes S, Piques M, Gibon Y. 2011. Water deficits uncouple growth from photosynthesis, increase C content, and modify the relationships between C and growth in sink organs. *Journal of Experimental Botany* **62**: 1715–1729.

Nakagawa S, Schielzeth H. 2013. A general and simple method for obtaining R^2 from generalized linear mixed-effects models. *Methods in Ecology and Evolution* **4**: 133–142.

O'Brien RM. 2007. A caution regarding rules of thumb for variance inflation factors. *Quality & Quantity* **41**: 673–690.

Oleksyn J, Zytkowiak R, Karolewski P, Reich PB, Tjoelker MG. 2000. Genetic and environmental control of seasonal carbohydrate dynamics in trees of diverse *Pinus sylvestris* populations. *Tree Physiology* **20**: 837–847.

Pan Y, Birdsey R, Fang JY, Houghton R, Kauppi PE, Kurz WA, Phillips OL, Shvidenko A, Lewis SL, Canadell JG *et al.* 2011. A large and persistent carbon sink in the world's forests. *Science* **333**: 988–993.

Peng CH, Liu JX, Dang QL, Apps MJ, Jiang H. 2002. TRIPLEX: a generic hybrid model for predicting forest growth and carbon and nitrogen dynamics. *Ecological Modelling* **153**: 109–130.

Pinheiro JC, Bates DM. 2000. *Mixed-effects models in S and S-PLUS*. New York, NY, USA: Springer.

Poorter H, Navas ML. 2003. Plant growth and competition at elevated CO_2: on winners, losers and functional groups. *New Phytologist* **157**: 175–198.

Rossi S, Anfodillo T, Menardi R. 2006a. Trephor: a new tool for sampling microcores from tree stems. *IAWA Journal* **27**: 89–97.

Rossi S, Deslauriers A, Anfodillo T, Morin H, Saracino A, Motta R, Borghetti M. 2006b. Conifers in cold environments synchronize maximum growth rate of tree-ring formation with day length. *New Phytologist* **170**: 301–310.

Rossi S, Rathgeber C, Deslauriers A. 2009. Comparing needle and shoot phenology with xylem development on three conifer species in Italy. *Annals of Forest Science* **66**: 206.

Savidge RA. 1988. Auxin and ethylene regulation of diameter growth in trees. *Tree Physiology* **4**: 401–414.

Sheridan SC. 2002. The redevelopment of a weather-type classification scheme for North America. *International Journal of Climatology* **22**: 51–68.

Singer JD. 1998. Using SAS Proc Mixed to fit multilevel models, hierarchical models, and individual growth models. *Journal of Educational and Behavioral Statistics* **24**: 323–355.

Sorce C, Giovannelli A, Sebastiani L, Anfodillo T. 2013. Hormonal signals involved in the regulation of cambial activity, xylogenesis and vessel pattering in trees. *Plant Cell Report* **32**: 885–898.

Uggla C, Mellerowicz EJ, Sundberg B. 1998. Indole-3-acetic acid controls cambial growth in Scots pine by positional signaling. *Plant Physiology* **117**: 113–121.

Warren WG. 1980. On removing the growth trend from dendrochronological data. *Tree-Ring Bulletin* **40**: 35–44.

Zeeman SC, Smith SM, Smith AM. 2007. The diurnal metabolism of leaf starch. *Biochemical Journal* **401**: 13–28.

Zhai LH, Bergeron Y, Huang JG, Berninger F. 2012. Variation in intra-annual wood formation, and foliage and shoot development of three major Canadian boreal tree species. *American Journal of Botany* **99**: 827–837.

Supporting Information

Additional supporting information may be found in the online version of this article.

Fig. S1 Gompertz function-based predictions of primary and secondary growth for spruce and fir over the growing seasons across the sites.

Fig. S2 Hugershoff function-based predictions of cambium activity for spruce and fir over the growing seasons across the sites.

Fig. S3 Schematic representation of the study design used to build the mixed-effects model.

Fig. S4 Mixed-effects model-building process.

Fig. S5 Residuals against the xylem cell number predicted by the full model for spruce and fir.

Table S1 Statistics for the Gompertz function fit for xylem cell number, bud phenology stages, and shoot and needle length for spruce and fir over the growing seasons across the sites

Table S2 Statistics for the Hugershoff function fit for cambium cell number for spruce and fir over the growing seasons across the sites

Methods S1 Determination of the onset and termination of primary and secondary growth with the Gompertz and Hugershoff functions.

Methods S2 Detailed statistical approaches used during the mixed-effects model-building process.

Methods S3 Calculation equations for the marginal and conditional R^2 of a mixed-effects model and of the proportion change in variance.

Please note: Wiley Blackwell are not responsible for the content or functionality of any supporting information supplied by the authors. Any queries (other than missing material) should be directed to the *New Phytologist* Central Office.